J. Fluid Mech. (2002), *vol.* 454, *pp.* 1–20.
DOI: 10.1017/S0022112001007455 Printed in the United Kingdom

Modelling the morning glory of the Gulf of Carpentaria

By ANNE PORTER† AND NOEL F. SMYTH

Department of Mathematics and Statistics, The King's Buildings, University of Edinburgh, Edinburgh EH9 3JZ, Scotland, UK
e-mail: noel@maths.ed.ac.uk

(Received 17 December 1999 and in revised form 19 March 2001)

The morning glory is a meteorological phenomenon which occurs in northern Australia and takes the form of a series of roll clouds. The morning glory is generated by the interaction of nocturnal seabreezes over Cape York Peninsula and propagates in a south-westerly direction over the Gulf of Carpentaria. In the present work, it is shown that the morning glory can be modelled by the resonant flow of a two-layer fluid over topography, the topography being the mountains of Cape York Peninsula. In the limit of a deep upper layer, the equations of motion reduce to a forced Benjamin–Ono equation. In this context, resonant means that the underlying flow velocity of the seabreezes is near a linear long-wave velocity for one of the long-wave modes. The morning glory is then modelled by the undular bore (simple wave) solution of the modulation equations for the Benjamin–Ono equation. This modulation solution is compared with full numerical solutions of the forced Benjamin–Ono equation and good agreement is found when the wave amplitudes are not too large. The reason for the difference between the numerical and modulation solutions for large wave amplitude is also discussed. Finally, the predictions of the modulation solution are compared with observational data on the morning glory and good agreement is found for the pressure jump due to the lead wave of the morning glory, but not for the speed and half-width of this lead wave. The reasons for this are discussed.

1. Introduction

The morning glory is the name given to a frequently occurring meteorological phenomenon in the Gulf Country (Gulf of Carpentaria) and adjacent southern Cape York Peninsula of north Queensland, Australia (see maps of figure 1). It takes the form of a spectacular roll cloud, or series of such clouds, which have a typical width of about 4 km and reach heights of more than 2 km from a base level of a few hundred metres (Christie 1989). Morning glories often retain their identities for several hours and can extend in length from several to hundreds of kilometres (Christie 1992). Most of the observations of morning glories have been made in the region of the town of Burketown (see figure 1) in the Gulf Country of north Queensland (Christie 1992). It is observed that it propagates from a north-easterly direction and originates over Cape York Peninsula. Clarke, Smith & Reid (1981) found that the origin of the morning glory is the collision of opposing seabreezes from the Coral Sea and Gulf of Carpentaria over Cape York Peninsula in the early evening. Shortly after

† Present address: Department of Mathematics, University of Bristol, University Walk, Bristol BS8 1TW, UK.

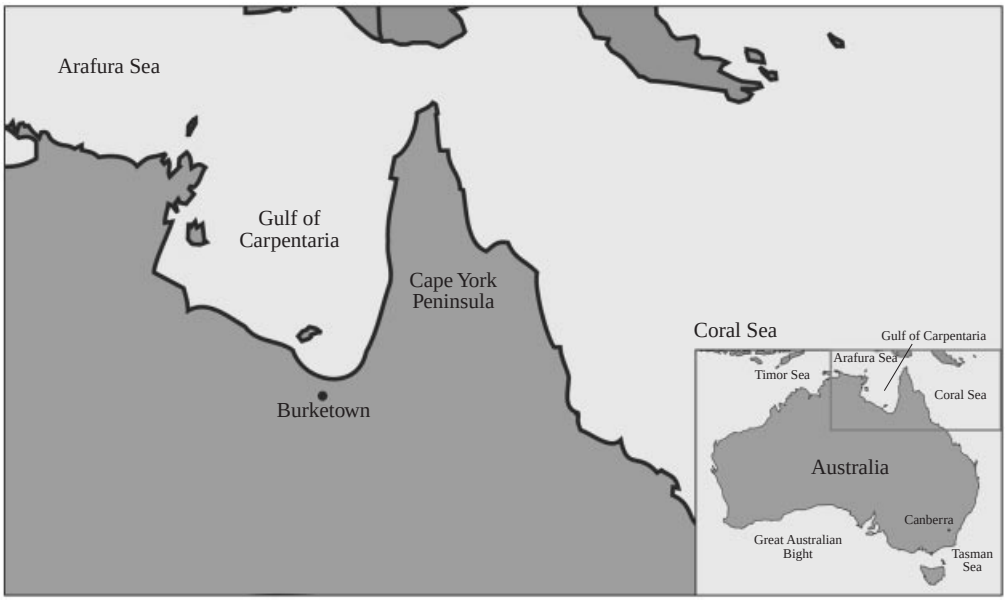

FIGURE 1. Map of Australia, with detail showing the locations of the Gulf of Carpentaria, Cape York Peninsula and Burketown, Queensland.

these breezes collide, large disturbances in the form of one or more solitary waves with amplitudes between 700 and 1000 m develop, followed by a decelerating gravity current. The disturbance propagates into the southern Gulf region and is then known as a morning glory. The spectacular roll clouds are formed at the leading edge of the solitary wave(s) as it lifts moist ambient air to the condensation level. After the cloud has dissolved, the glory can often continue to propagate for large distances (Christie 1992). Indeed, morning glories have been observed to propagate inland from Burketown over northwest Queensland for at least 300 km. Furthermore, some morning glories have been found to excite waves on an upper-level waveguide which have been detected the following night at Warramunga near Tennant Creek in the Northern Territory, which is approximately 1000 km from their origin in Cape York Peninsula. It is possible to have cloudless morning glories, and such nonlinear wave disturbances have been observed in other parts of Australia. The Gulf Country of Queensland is particularly suitable for cloud formation to be associated with the morning glory due to the humid air of the region.

The first detailed measurements of the morning glory were made by Clarke (1972). On the basis of simple numerical calculations, he described the phenomenon as a propagating hydraulic jump which originated in the highlands of Cape York Peninsula. Clarke's work precipitated much further study of morning glories and a decade of expeditions to the Gulf Country. As a result of their own measurements, Christie, Muirhead & Hales (1979) described the morning glory as due to a fairly well-developed, large-amplitude solitary wave or series of solitary waves. As a result of further measurements, Clarke *et al.* (1981) described it as an internal undular bore propagating on the shallow nocturnal boundary layer, in agreement with the results of Christie *et al.* (1979). Clarke (1983*a*, *b*) determined that the necessary conditions for the formation of a morning glory are: (i) a low-altitude dry peninsula from 150 to 500 km in width, (ii) opposing seabreezes from either side of the peninsula and

(iii) air dry enough to restrict much cloud development and moist enough in the lower layers for cloud lines to form. However subsequent numerical work by Smith & Noonan (1998) suggested that the morning glory is forced by a mesoscale convergence associated with the seabreezes over Cape York Peninsula and that the collision of the east and west coast seabreezes is not necessary for its formation. Detailed accounts of the work on morning glories are given in the review articles by Smith (1988) and Christie (1992).

The atmosphere in which the morning glory propagates can be approximated by a surface-based, stable lower layer in contact with the surface of the Earth lying below a deep upper layer (Christie 1989, 1992). The morning glories then propagate on the surface-based layer. The appropriate equation describing long nonlinear wave propagation in such a waveguide is the Benjamin–Ono equation

$$\frac{\partial u}{\partial t} + 2u\frac{\partial u}{\partial x} + \mathrm{PV}\frac{1}{\pi}\int_{-\infty}^{\infty} \frac{u_{yy}}{y-x}\,\mathrm{d}y = 0 \tag{1.1}$$

(Benjamin 1967; Christie 1989, 1992), where PV refers to the principal value of the integral and u is the non-dimensional mode amplitude. As most morning glories originate over the mountains of Cape York Peninsula, the full equation describing them is the forced Benjamin–Ono equation (Grimshaw & Smyth 1986), the forcing being due to the mountains. There has been extensive work, both experimental and theoretical, on fluid flow forced by topography, much of which is summarized and put into context in Baines (1995). Of particular relevance here is the work on the forced Korteweg–de Vries equation

$$-\frac{\partial u}{\partial t} - \Delta\frac{\partial u}{\partial x} + 6u\frac{\partial u}{\partial x} + \frac{\partial^3 u}{\partial x^3} + \frac{\mathrm{d}G}{\mathrm{d}x} = 0, \tag{1.2}$$

as the solutions of this forced equation are qualitatively similar to those of the forced Benjamin–Ono equation. The forced Korteweg–de Vries equation arises when the upstream velocity of a stratified fluid is close to one of the linear long-wave speeds for one of the long-wave modes. In this case, the flow is said to be trans-critical or resonant (Grimshaw & Smyth 1986; Baines 1995) and energy cannot propagate away from a forcing, such as topography. The amplitudes of forced waves then grow and the flow becomes nonlinear (Grimshaw & Smyth 1986; Baines 1995). This results in the production of nonlinear waves which propagate upstream from the forcing, as verified in the experiments of Lee, Yates & Wu (1989). The forced Korteweg–de Vries equation (1.2) is non-dimensional. The parameter Δ is a de-tuning parameter, with $\Delta = 0$ representing exact linear resonance, i.e. the upstream flow speed equals the long-wave mode speed. The function $G(x)$ is due to the topographic forcing. Solutions of the forced Korteweg–de Vries equation and the forced version of the Benjamin–Ono equation (1.1) are similar and methods for the solution of the latter can be deduced from the solutions of the former.

Smyth (1987) used the modulation equations for the Korteweg–de Vries equation derived by Whitham (1965, 1974) to find approximate solutions of the forced Korteweg–de Vries equation (1.2). Modulation theory for the Korteweg–de Vries equation is based on a slowly varying periodic wave (cnoidal wave). Equations for the slowly varying parameters of the wavetrain, such as amplitude, wavelength and mean height, are then obtained from an averaged Lagrangian. The modulation equations for the Korteweg–de Vries equation form a third-order hyperbolic system whose characteristic velocities are the nonlinear counterparts of the linear group

velocity. Gurevich & Pitaevskii (1974) showed that a simple wave solution of these hyperbolic modulation equations is the undular bore solution of the Korteweg–de Vries equation. This simple wave solution was subsequently found to be in excellent agreement with full numerical solutions of the Korteweg–de Vries equation by Fornberg & Whitham (1978). Numerical solutions of the forced Korteweg–de Vries equation (1.2) showed that in a band around $\Delta = 0$, the flow upstream and downstream of the forcing consisted of modulated periodic waves (Grimshaw & Smyth 1986). Outside this band, the flow was similar to the linear case. Smyth (1987) used the simple wave solution of the modulation equations for the Korteweg–de Vries equation to construct solutions for the flow upstream and downstream of the forcing in the resonant band of Δ. These upstream and downstream solutions were suitably modified versions of the undular bore solution of Gurevich & Pitaevskii (1974). Essentially the undular bore solution was used, but was cut off so that the upstream solution did not propagate downstream of the forcing and vice versa. These upstream and downstream solutions were found to be in excellent agreement with full numerical solutions of the forced Korteweg–de Vries equation (1.2).

Dobrokhotov & Krichever (1991) derived the modulation equations for the n-phase periodic wave solution of the Benjamin–Ono equation. Jorge, Minzoni & Smyth (1999) then used these to derive approximate solutions of the Benjamin–Ono equation for three initial conditions, the one of interest here corresponding to the undular bore solution of the Benjamin–Ono equation. In the present work, this undular bore solution will be used to derive the upstream and downstream solutions of the forced Benjamin–Ono equation in the resonant regime in a similar manner to that of Smyth (1987) for the forced Korteweg–de Vries equation. These approximate solutions will then be compared with full numerical solutions of the forced Benjamin–Ono equation and good agreement is found when the wave amplitudes are not high. The reason for the difference between the numerical and approximate solutions for high wave amplitudes is discussed. Finally the approximate modulation theory solutions are compared with the observational data of Christie (1989, 1992) and Menhofer *et al.* (1997) for the morning glory, which is modelled by the upstream modulated wavetrain. Good agreement is found for the pressure jump due to the arrival of the lead wave of the morning glory, but not for the speed and half-width of this wave. A number of reasons for this disagreement are discussed, the most important one being that the forcing height to waveguide depth ratio is too large for the weakly nonlinear Benjamin–Ono theory to be strictly valid. Similar disagreement between weakly nonlinear Benjamin–Ono theory and observational data was found by Noonan & Smith (1985) for much the same reasons. However the present work gives an explicit theory which enables the wave properties to be calculated from the forcing (mountains) which generates these waves. This was not done by Noonan & Smith (1985) as they only modelled the morning glory in the region in which the observational measurements were made, this region being far from the generation region. Furthermore, they modelled the morning glory by a Benjamin–Ono soliton, rather than the modulated wave (undular bore) of the present work. The present theory predicts that in the weakly nonlinear limit the flow of the coastal seabreeze over the mountains of Cape York Peninsula is resonant (trans-critical). Therefore while an accurate model of the morning glory will require numerical integration of the governing equations, the weakly nonlinear theory does indicate that the topographic forcing will have a greater effect on the generation of the morning glory than would otherwise be the case. This topographic effect has not been considered in previous work.

2. Forced Benjamin–Ono equation

As discussed by Christie (1989), the morning glory is a long, nonlinear wave disturbance which is confined to a surface-based waveguide which has a typical depth of 500 m (Christie 1989, 1992). Above this surface waveguide there is a deep, upper, neutrally stable layer of typical depth 4 km (Christie 1989; Menhofer *et al.* 1997). For such waves the appropriate length scale h is the effective depth of the waveguide, rather than the total fluid depth, as for the Korteweg–de Vries equation. The waves making up the morning glory have typical wavelengths of 10–20 km (Noonan & Smith 1985; Menhofer *et al.* 1997) and typical half-widths of 2 km (Noonan & Smith 1985). The wavefront of the morning glory can extend anywhere from 200 km to 1000 km in length and is basically straight (Christie 1992). Since the wave-length to front length ratio is then small, the morning glory can be modelled as two-dimensional. The equation governing two-dimensional, long-wavelength, weakly nonlinear disturbances in a two-layer stratified fluid for which one of the layers is a deep, neutrally stable layer is the Benjamin–Ono equation (Benjamin 1967). Let us then consider the two-dimensional flow of a density-stratified, inviscid fluid in a waveguide of depth h which lies underneath a deep upper layer for the case in which the fluid in the waveguide has velocity U at upstream infinity. Let us further assume that the topographic forcing is localized. We take the coordinate Z to be orientated vertically upwards, with $Z = 0$ being the flat ground away from the topography, and the X-coordinate to be orientated in the direction of the upstream flow, with $X = 0$ being some point in the topography. The displacement $\eta(X, Z, T)$ of the fluid is then given by

$$\eta(X, Z, T) = A(X, T)\phi(Z), \tag{2.1}$$

where $\phi(Z)$ is the modal function. The amplitude $A(X, T)$ is in turn determined by the forced Benjamin–Ono equation

$$-\frac{\partial A}{\partial T} - \delta\frac{\partial A}{\partial X} + \alpha A\frac{\partial A}{\partial X} + \beta \mathrm{PV}\frac{1}{\pi}\int_{-\infty}^{\infty}\frac{A_{YY}}{Y - X}\,\mathrm{d}Y + \frac{c_n}{2}\frac{\mathrm{d}G(X)}{\mathrm{d}X} = 0 \tag{2.2}$$

for the case in which the underlying velocity U is close to the modal velocity c_n (Grimshaw & Smyth 1986). The parameters α and β are related to the density stratification in the waveguide (Grimshaw & Smyth 1986; Christie 1989), $\delta = U - c_n$ and $G(x)$ is the topographic profile. The parameter Δ thus measures how close the flow is to exact linear resonance and is thus a 'de-tuning' parameter. The forced Benjamin–Ono equation (2.2) can be put into non-dimensional form via the transformations

$$X = hx, \quad T = \frac{h^2}{\beta}t, \quad A = \frac{2\beta}{\alpha h}u. \tag{2.3}$$

Using these transformations, the forced Benjamin–Ono equation (2.2) becomes

$$-\frac{\partial u}{\partial t} - \Delta\frac{\partial u}{\partial x} + 2u\frac{\partial u}{\partial x} + \mathrm{PV}\frac{1}{\pi}\int_{-\infty}^{\infty}\frac{u_{yy}}{y - x}\,\mathrm{d}y + \frac{\mathrm{d}g(x)}{\mathrm{d}x} = 0, \tag{2.4}$$

where

$$\Delta = \frac{h}{\beta}\delta \quad \text{and} \quad g = \frac{\alpha h^2 c_n}{4\beta^2}G. \tag{2.5}$$

Away from the forcing, the forced Benjamin–Ono equation (2.4) is the standard Benjamin–Ono equation

$$-\frac{\partial u}{\partial t} - \Delta\frac{\partial u}{\partial x} + 2u\frac{\partial u}{\partial x} + \mathrm{PV}\frac{1}{\pi}\int_{-\infty}^{\infty}\frac{u_{yy}}{y - x}\,\mathrm{d}y = 0. \tag{2.6}$$

The single-phase periodic wave solution of the Benjamin–Ono equation (2.6) is

$$u = c + a - b + 2(b-a)\frac{b - c - \sqrt{(b-c)(a-c)}\cos\phi}{a + b - 2c - 2\sqrt{(b-c)(a-c)}\cos\phi}, \tag{2.7}$$

with the phase ϕ being

$$\phi(x,t) = \Delta - (a-b)x - (a^2 - b^2)t \tag{2.8}$$

(Dobrokhotov & Krichever 1991). The mean level m of this periodic solution is

$$m = \frac{1}{2\pi}\int_0^{2\pi} u(x,t)\,\mathrm{d}\phi = c + b - a \tag{2.9}$$

and its amplitude S is

$$S = 4\sqrt{(b-c)(a-c)}. \tag{2.10}$$

The periodic solution has two limits of interest: $a \to b$, which gives the soliton solution; and $a \to c$, which gives the linear solution. Taking the soliton limit $a \to b$, the periodic solution becomes

$$u = c + 4\frac{b-c}{1 + 4(b-c)^2(x - 2bt)^2}, \tag{2.11}$$

which is the soliton solution of the Benjamin–Ono equation, of amplitude

$$A_s = 4(b-c). \tag{2.12}$$

In the linear limit $a \to c$, the periodic solution (2.7) becomes the small-amplitude periodic wave

$$u = b + 2\sqrt{\frac{a-c}{b-c}}(b-a)\cos\phi. \tag{2.13}$$

Modulation theory for the Benjamin–Ono equation is now constructed by allowing the parameters a, b and c in the periodic wave solution (2.7) to slowly vary in x and t. Dobrokhotov & Krichever (1991) showed that the modulation equations for these periodic wave parameters in characteristic form are

$$\left.\begin{aligned} a = \text{constant} \quad &\text{on} \quad \frac{\mathrm{d}x}{\mathrm{d}t} = \Delta - 2a, \\ b = \text{constant} \quad &\text{on} \quad \frac{\mathrm{d}x}{\mathrm{d}t} = \Delta - 2b, \\ c = \text{constant} \quad &\text{on} \quad \frac{\mathrm{d}x}{\mathrm{d}t} = \Delta - 2c. \end{aligned}\right\} \tag{2.14}$$

The modulation equations for the Benjamin–Ono equation then decouple, so that they are easy to solve, unlike those for the Korteweg–de Vries equation (Whitham 1965, 1974). Jorge *et al.* (1999) considered the initial condition

$$u(x,0) = \begin{cases} 0, & x < 0 \\ B, & x > 0 \end{cases} \tag{2.15}$$

for the Benjamin–Ono equation, where $B > 0$ is a constant. They showed that an approximate solution of the Benjamin–Ono equation (2.6) for this initial condition

could be found by solving the modulation equations (2.14) with $b = B$, $c = 0$ and

$$a(x,0) = \begin{cases} B, & x < 0 \\ 0, & x > 0. \end{cases} \tag{2.16}$$

The modulation solution is then a simple wave solution of the modulation equations and is

$$a(x,t) = \begin{cases} B, & x < (\Delta - 2B)t \\ \frac{1}{2}\left(\Delta - (x/t)\right), & (\Delta - 2B)t \leqslant x \leqslant \Delta t \\ 0, & x > \Delta t, \end{cases} \tag{2.17}$$

with $b = B$ and $c = 0$. The approximate solution of the Benjamin–Ono equation (2.6) is then found by substituting these values for a, b and c into the periodic solution (2.7). Jorge *et al.* (1999) showed that this approximate modulation solution corresponds to an undular bore solution, which is the dispersive resolution of the step initial condition (2.15). This solution is a modulated periodic wave which approaches solitons at its leading edge $x = (\Delta - 2B)t$ and linear waves at its trailing edge $x = \Delta t$. Jorge *et al.* (1999) found that the approximate undular bore solution is in excellent agreement with full numerical solutions of the Benjamin–Ono equation (2.6) for the initial condition (2.15). We see from the soliton amplitude (2.12) that the lead soliton amplitude of the bore is 4 times the initial jump height (since $b = B$). This amplitude relation for an undular bore was noted by Christie (1989, 1992) from full numerical solutions of the Benjamin–Ono equation. It is modifications of this undular bore solution which will be used to construct approximate solutions of the forced Benjamin–Ono equation (2.4).

3. Approximate solutions

Approximate solutions of the forced Benjamin–Ono equation (2.4) for the flow upstream and downstream of the topography will now be found using simple wave solutions of the modulation equations (2.14) for the Benjamin–Ono equation. These approximate upstream and downstream solutions are similar to those derived for the forced Korteweg–de Vries equation by Smyth (1987). In § 5, the approximate solutions will be compared with full numerical solutions of the forced Benjamin–Ono equation (2.4) obtained using the pseudo-spectral method of Fornberg & Whitham (1978). As a particular localized forcing, the profile

$$g = g_0 \mathrm{sech}^2 wx \tag{3.1}$$

was used in the numerical solutions. Also it is assumed that there is no disturbance initially, so that

$$u(x,0) = 0, \quad -\infty < x < \infty. \tag{3.2}$$

Figure 2(a) shows the evolution of the numerical solution of the forced Benjamin–Ono equation (2.4) for the parameter values $\Delta = 0$, $g_0 = 2$ and $w = 0.1$. It can be seen that there are distinct upstream and downstream wavetrains linked by a steady profile over the topography and that both the upstream and downstream wavetrains have the form of undular bores. The upstream wavetrain forced by the topography corresponds to the morning glory. Indeed, Christie (1989, 1992) observed that in many cases the morning glory took the form of an undular bore. The solution of the forced Benjamin–Ono equation is qualitatively similar to that of the forced Korteweg–de Vries equation (Grimshaw & Smyth 1986; Smyth 1987), as is expected since the

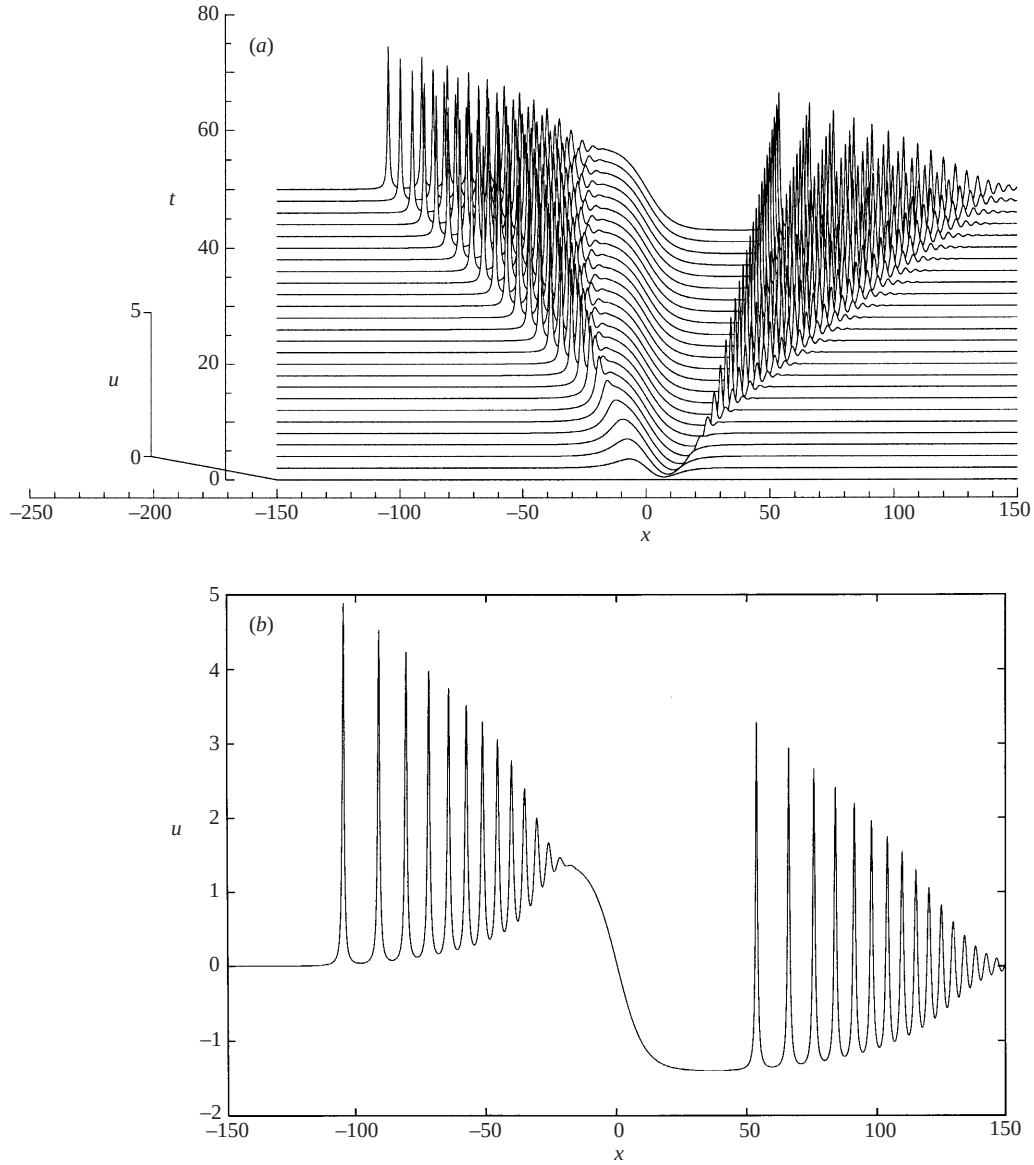

FIGURE 2. (*a*) Evolution of the solution of the forced Benjamin–Ono equation (2.4) for $\Delta = 0$ and $g = 2\,\mathrm{sech}^2 0.1x$. The time t for each individual solution is shown on the vertical axis labelled with t. The amplitude scale for u is shown on the vertical axis on the left-hand side. (*b*) Numerical solution of the forced Benjamin–Ono equation (2.4) at $t = 50$ for $\Delta = 0$ and $g = 2\,\mathrm{sech}^2 0.1x$.

main difference between the Benjamin–Ono and Korteweg–de Vries equations is the dispersion relation. The obvious difference between the upstream and downstream bores is that the upstream bore is from the undisturbed level, while the downstream bore rises from the negative depression on the downstream side of the forcing. These upstream and downstream flows will now be found as simple wave solutions of the modulation equations (2.14). The modulation equations for the unforced Benjamin–Ono equation (2.6) can be used to construct the upstream and downstream solutions for the forced Benjamin–Ono equation (2.4) since the forcing is localized.

The upstream and downstream wavetrains propagate away from the forcing, in which region the modulation equations (2.14) are appropriate.

3.1. *Upstream solution*

Let us first derive the approximate solution for the upstream wavetrain. As the upstream bore has solitons at its leading edge, $a \to b$ at the leading edge. It is therefore apparent from the mean level expression (2.9) that for the upstream bore to rise from the undisturbed level we require $c = 0$. The upstream solution is then the simple wave solution $b = B_-$ and

$$a = \begin{cases} B_-, & x < (\Delta - 2B_-)t \\ \frac{1}{2}(\Delta - (x/t)), & (\Delta - 2B_-)t \leqslant x \leqslant \Delta t \\ 0, & \Delta t < x \leqslant 0 \end{cases} \tag{3.3}$$

of the modulation equations (2.14), where $B_- > 0$. This bore solution gives a smooth jump from the mean level 0 to the mean level B_-. It is noted that the trailing edge of the wavetrain is $x = \Delta t$. Since the upstream wavetrain must propagate into $x < 0$ only, the solution (3.3) is valid for $\Delta \leqslant 0$. For $\Delta > 0$, the upstream simple wave solution must be terminated at $x = 0$ so that it does not partly propagate downstream, as was done by Smyth (1987) for the equivalent upstream solution of the forced Korteweg–de Vries equation (1.2). The upstream simple wave solution for $\Delta > 0$ is therefore

$$a = \begin{cases} B_+, & x < (\Delta - 2B_+)t \\ \frac{1}{2}(\Delta - (x/t)), & (\Delta - 2B_+)t \leqslant x \leqslant 0, \end{cases} \tag{3.4}$$

where $B_+ > 0$.

3.2. *Downstream solution*

The solution downstream of the forcing (topography) can be similarly found as a simple wave solution of the modulation equations (2.14). As can be seen from figure 2(*a*), the main difference between the upstream and downstream solutions is that the downstream solution jumps from a negative mean level to the undisturbed level. Now the leading edge of the downstream bore consists of linear waves. As the linear wave limit of the periodic solution has $a \to c$, we see from the mean level expression (2.9) that we require $b = 0$ for the leading edge to approach the undisturbed level. The downstream wavetrain is therefore the simple wave solution $b = 0$, $c = C_+$ and

$$a = \begin{cases} 0, & 0 \leqslant x < \Delta t \\ \frac{1}{2}(\Delta - (x/t)), & \Delta t \leqslant x \leqslant (\Delta - 2C_+)t \\ C_+, & x > (\Delta - 2C_+)t \end{cases} \tag{3.5}$$

of the modulation equations (2.14), where $C_+ < 0$. This downstream bore solution gives a jump from the negative mean level C_+ to 0. As for the upstream simple wave solution for $\Delta \geqslant 0$, the simple wave solution (3.5) will partly propagate upstream when $\Delta < 0$. Hence as for the upstream solution, the simple wave solution is truncated at $x = 0$ when $\Delta < 0$, as was done by Smyth (1987) in the corresponding case for the downstream solution of the forced Korteweg–de Vries equation (1.2). The downstream simple wave solution for $\Delta < 0$ is then $b = 0$, $c = C_-$ and

$$a = \begin{cases} \frac{1}{2}(\Delta - (x/t)), & 0 \leqslant x \leqslant (\Delta - 2C_-)t \\ C_-, & x > (\Delta - 2C_-)t, \end{cases} \tag{3.6}$$

where $C_- < 0$.

The upstream and downstream solutions are now complete, except for the constants B_-, B_+, C_- and C_+, which give the size of the jumps across the simple waves. Approximate values of these constants will now be found by matching across the forcing in a similar manner to that employed by Smyth (1987). The upstream and downstream solutions have been derived from the modulation equations for the unforced Benjamin–Ono equation, so that there still needs to be some linkage to the forcing. This linkage is through the constants B_-, B_+, C_- and C_+.

4. Bore constants

From figure 2(a) it can be seen that the flow over the forcing is steady, even though the upstream and downstream wavetrains are not. This steady flow is the solution of

$$-\Delta\frac{\partial u}{\partial x}+2u\frac{\partial u}{\partial x}+\mathrm{PV}\frac{1}{\pi}\int_{-\infty}^{\infty}\frac{u_{yy}}{y-x}\,\mathrm{d}y+\frac{\mathrm{d}g(x)}{\mathrm{d}x}=0. \tag{4.1}$$

As in Smyth (1987), let us consider the limit of a broad forcing, which in the case of the morning glory means that we are assuming that the length scale of the topographic forcing is much larger than the depth of the lower waveguide, which typically is 500 m Christie (1989, 1992). This assumption is reasonable for the length scales of mountain ranges. In the limit of a broad forcing, the dispersive term in the steady equation (4.1) is negligible, so that the steady flow over a broad forcing is governed by

$$-\Delta\frac{\partial u}{\partial x}+2u\frac{\partial u}{\partial x}+\frac{dg(x)}{dx}=0. \tag{4.2}$$

The solution of this steady equation which is continuous at $x=0$ and has the correct sign upstream and downstream is

$$u_s=\begin{cases}\frac{1}{2}\Delta+\sqrt{g_0-g(x)}, & x\leqslant 0\\ \frac{1}{2}\Delta-\sqrt{g_0-g(x)}, & x\geqslant 0,\end{cases} \tag{4.3}$$

where $g_0=g(0)$. The simple wave solutions of the previous section will now be matched to this steady solution over the forcing. In this regard, we note that

$$u_s=\begin{cases}\frac{1}{2}\Delta+\sqrt{g_0}, & x\to-\infty\\ \frac{1}{2}\Delta-\sqrt{g_0}, & x\to\infty,\end{cases} \tag{4.4}$$

since the forcing is assumed to be localized.

Since the resonant flow has been assumed to have been generated from the rest state, the steady solutions (4.3) and the matching of the upstream and downstream solutions to these steady states undertaken in the next subsections cannot be uniformally valid from $t=0$. This matching then gives the long-time resonant solution after the transients generated by the formation of the flow from the rest state have died out. In the present work we shall not be interested in the short-term start-up process and from figure 2(a) it can be seen that the generation of the modulated upstream and downstream wavetrains is relatively rapid. Indeed the generation of the steady state (4.3) from the initial rest state can be clearly seen in this figure.

4.1. *Upstream matching*

The upstream modulation solution has distinct forms, depending on whether the de-tuning parameter Δ is positive or negative. Let us first consider the simpler case in which $\Delta\leqslant 0$. The upstream modulation solution (3.3) for $\Delta\leqslant 0$ has $c=0$ and

$b = B_-$. The mean level expression (2.9) and modulation solution (3.3) then give that the modulated wave has the mean level $m = b = B_-$ at the trailing edge. Matching with the steady solution (4.4) over the forcing, we thus have that

$$B_- = \tfrac{1}{2}\Delta + \sqrt{g_0}. \tag{4.5}$$

The determination of the upstream constant B_+ for $\Delta > 0$ is more problematical. It can be seen from the upstream solution (3.4) for $\Delta > 0$ that the wavetrain does not approach a constant at its trailing edge and waves are continually generated just upstream of the forcing, as can be seen in figure 4(*a*) below. The matching between the steady solution over the forcing and the modulation solution therefore cannot be done as for $\Delta \leqslant 0$. To overcome this, the matching between the modulation solution and the steady solution over the forcing is made in the mean, as was done by Smyth (1987) for the equivalent case for the forced Korteweg–de Vries equation. Modulation theory determines the slowly varying properties of an underlying oscillation. It can therefore be used only to determine the properties of a wavetrain averaged over a number of wavelengths and so cannot be used to match values at a fixed point. Smyth (1987) found that the modulation solution determined using this matching in the mean was in good agreement with full numerical solutions of the forced Korteweg–de Vries equation. It can be seen from the modulation solution (3.4) that $a = \Delta/2$ at $x = 0$. Since $c = 0$ and $b = B_+$, we have from the mean level expression (2.9) that the mean level of the modulation solution at $x = 0$ is

$$m = B_+ - \tfrac{1}{2}\Delta. \tag{4.6}$$

Matching this mean level with the steady solution (4.4) over the forcing gives

$$B_+ = \Delta + \sqrt{g_0}. \tag{4.7}$$

4.2. *Downstream matching*

The matching between the steady solution over the forcing and the downstream modulation solution is performed in exactly the same manner as for the upstream solution. For $\Delta \geqslant 0$ the downstream modulation solution (3.5) approaches a constant level C_+ at its trailing edge. Matching this value with the steady solution (4.4) over the forcing gives

$$C_+ = \tfrac{1}{2}\Delta - \sqrt{g_0}, \tag{4.8}$$

on using the mean level expression (2.9).

The downstream solution (3.6) for $\Delta < 0$ does not approach a constant value at its trailing edge at $x = 0$ and so has to be matched in the mean as for the upstream solution for $\Delta > 0$. The downstream solution has $b = 0$ and from the solution (3.6) for a it can be seen that $a = \Delta/2$ at $x = 0$. Hence from (2.9) the mean level of the downstream solution at $x = 0$ is

$$m = C_- - \tfrac{1}{2}\Delta \tag{4.9}$$

and so matching with the steady solution (4.4) over the forcing gives

$$C_- = \Delta - \sqrt{g_0}. \tag{4.10}$$

The constants B_- and B_+ must be positive and the constants C_- and C_+ must be negative, by construction. It can therefore be seen from (4.5), (4.7), (4.8) and (4.10) that the modulation solution is valid for

$$-2\sqrt{g_0} < \Delta < 2\sqrt{g_0}. \tag{4.11}$$

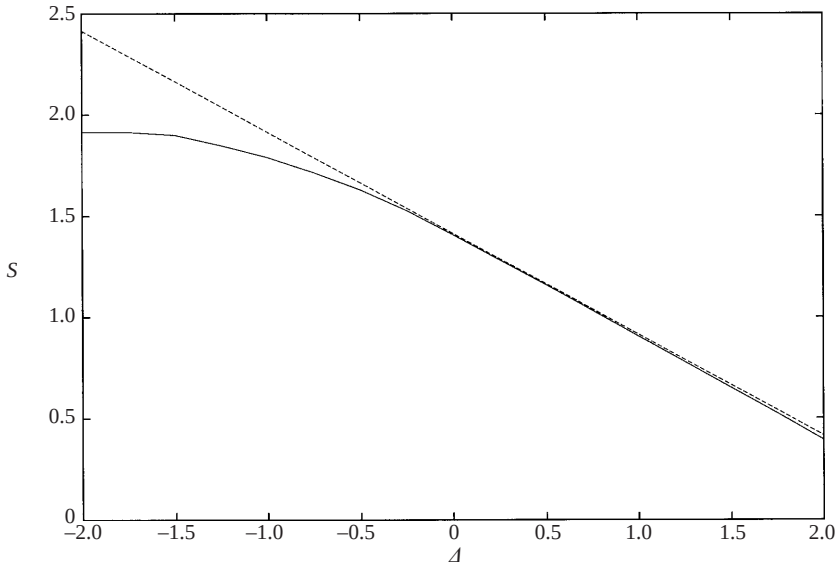

FIGURE 3. Depth S of shelf downstream of forcing for $\Delta \geqslant 0$. ——, Numerical solution of forced Benjamin–Ono equation; – – –, steady solution (4.4). The forcing (3.1) was used with $g_0 = 2$ and $w = 0.1$.

Outside this range, the flow is qualitatively similar to the linear solution (Grimshaw & Smyth 1986; Smyth 1987) in that there is no large, permanent upstream disturbance. This band of Δ is the resonant or trans-critical range for flow over the forcing.

5. Comparison with numerical solutions

The modulation solutions of the previous two sections will now be compared with full numerical solutions of the forced Benjamin–Ono equation (2.4) obtained using the pseudo-spectral method of Fornberg & Whitham (1978). In the next section, the modulation solution will be compared with observational data.

The modulation solutions of § 3 were completed in § 4 by matching with the steady solution over the forcing. On the downstream side of the forcing, this steady solution approaches a flat shelf. This downstream shelf can be clearly seen in figure 2(b), which shows the full numerical solution of the forced Benjamin–Ono equation (2.4) for $\Delta = 0$ at $t = 50$. From the limit (4.4) of the steady solution as $x \to \infty$, the depth of this shelf is

$$S = \tfrac{1}{2}\Delta - \sqrt{g_0}. \tag{5.1}$$

The validity of the assumption of a steady flow over the forcing can be tested via this shelf. Figure 3 shows a comparison between the depth of the shelf downstream of the forcing as given by the full numerical solution of the forced Benjamin–Ono equation (2.4) and by (5.1). It can be seen that the agreement is excellent for $\Delta \geqslant 0$. For $\Delta < 0$ the expression (5.1) progressively over-estimates the depth of the shelf as Δ decreases. The reason for this is that as Δ decreases the downstream wavetrain starts closer and closer to the forcing, so that the asymptotic state (5.1) becomes a less accurate approximation to the depth of the shelf. However in the present work, we shall mainly be interested in values of Δ between approximately $-\sqrt{g_0}$ and 0, in which case the depth (5.1) is still an accurate approximation.

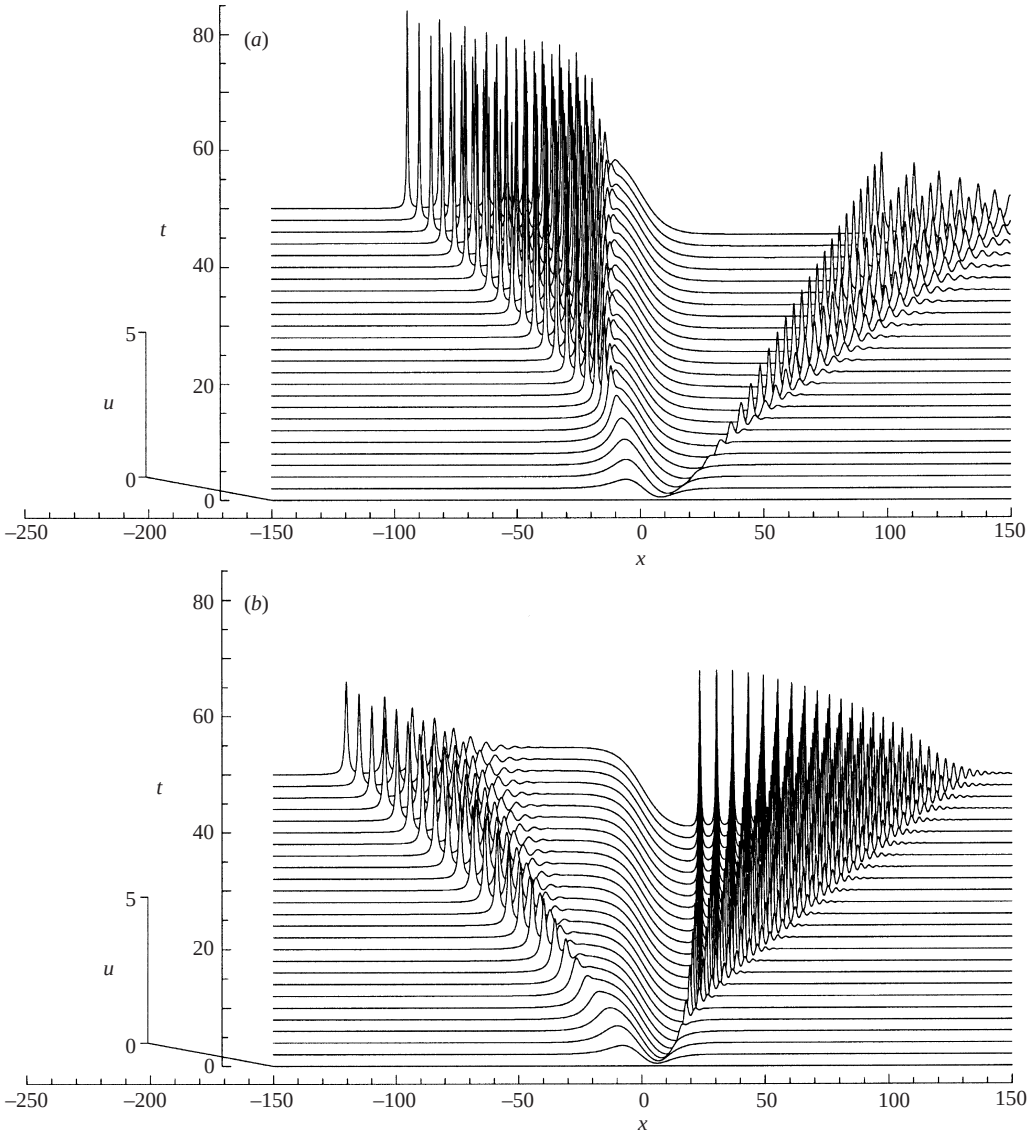

FIGURE 4. Evolution of the numerical solution of the forced Benjamin–Ono equation (2.4) for $g_0 = 2.0$ and $w = 0.1$ The time t for each individual solution is shown on the vertical axis labelled with t. The amplitude scale for u is shown on the vertical axis on the left-hand side. (a) $\Delta = 1.0$, (b) $\Delta = -1.0$.

The modulation solutions (3.3) and (3.4) predict that the upstream wavetrain leaves the region of the forcing for $\Delta < 0$, while for $\Delta \geqslant 0$ waves are continually generated just upstream of the forcing. That this is indeed the case can be seen from the numerical solutions for $\Delta = 1$ and $\Delta = -1$ shown in figure 4. It can also be seen that the opposite is true for the downstream wavetrain, as predicted by the modulation solutions (3.5) and (3.6). The modulation solutions (3.5) and (3.6) predict that the downstream wavetrain propagates away from the forcing for $\Delta > 0$, but stays attached just downstream of the forcing for $\Delta \leqslant 0$, as is verified in figure 4.

The final comparison to be made between the numerical and modulation solutions

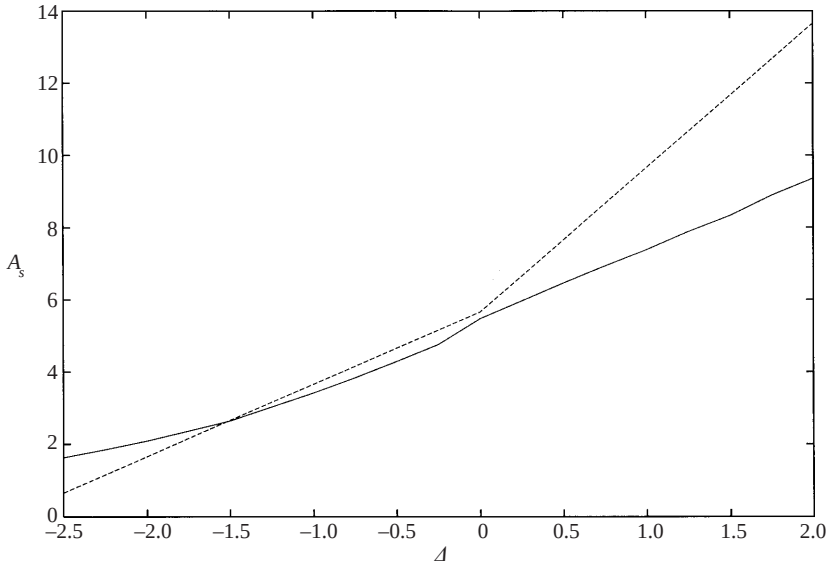

FIGURE 5. Amplitude A_s of the lead wave of the upstream wavetrain as a function of Δ. ——, Numerical solution of forced Benjamin–Ono equation (2.4); – – –, amplitude as given by modulation solution. The numerical solution used the forcing (3.1) with $g_0 = 2.0$ and $w = 0.1$.

is that for the amplitude of the lead wave of the upstream wavetrain. The modulation solutions (3.3) and (3.4) and the periodic wave amplitude (2.10) give that the amplitude A_s of the lead wave of the upstream wavetrain is

$$A_s = 4\Delta + 4\sqrt{g_0} \tag{5.2}$$

for $\Delta \geqslant 0$ and

$$A_s = 2\Delta + 4\sqrt{g_0} \tag{5.3}$$

for $\Delta < 0$. A comparison between the amplitude of the lead wave of the upstream wavetrain as given by the modulation solution and by the full numerical solution is shown in figure 5. It can be seen that there is good agreement around exact resonance at $\Delta = 0$. As the supercritical $\Delta = 2\sqrt{g_0}$ and subcritical $\Delta = -2\sqrt{g_0}$ limits of resonant flow are approached, the agreement between the numerical and approximate solutions decreases. For Δ near the supercritical limit, this discrepancy between the two solutions is due to the lead waves breaking up into two or more solitons due to their large amplitudes. A further point to note is that the agreement between the numerical and approximate solutions is expected to decrease away from exact resonance $\Delta = 0$ since as the supercritical $\Delta = 2\sqrt{g_0}$ and subcritical $\Delta = -2\sqrt{g_0}$ limits are approached the nature of the flow is changing. This can be seen in figure 5 as $\Delta = -2.5$ is approached. Similar behaviour was found for the forced Korteweg–de Vries equation by Grimshaw & Smyth (1986) and Smyth (1987).

6. Comparison with observational data

In this section the modulation solution of §§ 3 and 4 will be compared with the observational data of Christie (1989, 1992) and Menhofer *et al.* (1997) for the morning glory at various points around the Queensland coast of the Gulf of Carpentaria. To compare with these data, some assumptions will have to be made about the

stratification state of the atmosphere into which the morning glory propagates. As a model of the atmosphere, Christie (1989) assumed that the lower waveguide layer in which it propagates has depth h and a constant Brunt–Väisälä frequency N and that the upper layer is neutrally stable ($N = 0$). It was then shown that in the limit of a small density jump across the interface between the upper and lower layers, the coefficients in the dimensional Benjamin–Ono equation (2.2) are

$$\alpha = 4N/\pi, \tag{6.1}$$

$$\beta = 8Nh^2/\pi^3, \tag{6.2}$$

$$c_n = c_1 = 2Nh/\pi, \tag{6.3}$$

for a first mode wave. Using these parameter values and the non-dimensionalizations (2.5), the non-dimensional forcing height g_0 is then related to the dimensional height G_0 by

$$g_0 = \frac{\pi^4}{32h} G_0. \tag{6.4}$$

Christie (1989) gives that for this stratification, the pressure change ΔP due to a wave of dimensional height A is given as

$$\Delta P = \frac{2\rho h N^2}{\pi} A, \tag{6.5}$$

for air of density ρ. The non-dimensionalizations (2.3) then give that the pressure change is given in terms of the non-dimensional amplitude u by

$$\Delta P = \frac{8\rho h^2 N^2}{\pi^3} u. \tag{6.6}$$

The predictions of the pressure jump expression (6.6) can be compared with the observational data of Christie (1989, 1992) and Menhofer *et al.* (1997). Using the expression (5.3) for the amplitude of the lead wave of the upstream wavetrain for $\Delta \leqslant 0$, the pressure jump associated with this lead wave can be calculated via (6.6). The observational data of Christie (1989, 1992) and Menhofer *et al.* (1997) for the pressure jump of the lead wave of the morning glory are presented in table 1. These two sets of observational data are in broad agreement. Christie (1992) gives that the depth h of the waveguide layer varies between 400 m and 1200 m and that a typical value of the Brunt–Väisälä frequency is $N = 0.0233\,\mathrm{s}^{-1}$. Clarke (1983) and Christie (1992) found that the morning glory is generated in a region between 40 km and 70 km inland from the Gulf coast of Cape York Peninsula. This region is in the foothills of the mountains in Cape York Peninsula, where the mountains range between 100 m and 200 m in height, with most of the elevation being towards the lower end of this range. Numerical studies by Clarke (1984) found that atmospheric bores can be generated by colliding sea-breezes provided they have speeds less than $7\,\mathrm{m\,s}^{-1}$. The final piece of data needed is the density of the air in the waveguide, which can be taken to be $1.16\,\mathrm{kg\,m}^{-3}$ for a typical summer daytime temperature of 30 °C. Using these values, the pressure jump due to the lead wave of the upstream wavetrain as predicted by the modulation solution can be calculated via (6.6) and (5.3). The results are presented in table 2.

In table 2 the pressure jump as predicted by the modulation solution has been calculated for the case of exact resonance $\Delta = 0$ and for the subcritical value $\Delta = -\sqrt{g_0}$. It can be seen from tables 1 and 2 that the modulation solution predictions are in better agreement with the observations for the lower end of the range

Date	ΔP (hPa)
September, 1983 :C	0.55–0.81
October, 1983 :C	0.55–0.85
November, 1990 :C	1.23
7/9/91–6/10/91 :M	0.5–1.5

TABLE 1. Observations of pressure jump ΔP of the lead wave of the morning glory as given in Christie (1989, 1992) (C) and Menhofer *et al.* (1997) (M).

G_0 (m)	Δ	ΔP (hPa); $h = 400$ m	ΔP(hPa); $h = 500$ m	ΔP(hPa); $h = 1200$ m
100	0	0.91	1.27	4.71
100	$-\sqrt{g_0}$	0.45	0.63	2.36
150	0	1.11	1.55	5.77
150	$-\sqrt{g_0}$	0.56	0.78	2.89
200	0	1.28	1.80	6.67
200	$-\sqrt{g_0}$	0.64	0.89	3.33

TABLE 2. Pressure jump ΔP of the lead wave of an upstream wavetrain (morning glory) as given by the modulation solution for a range of mountain heights G_0.

of waveguide depths of 400 m and 500 m. In this regard, numerical calculations of Smith & Noonan (1998) of the atmospheric flow over the Gulf of Carpentaria–Cape York Peninsula–Coral Sea region show that over land a shallow stable layer of depth 500 m underlying a deep upper layer with weak vertical gradients forms during the night. Furthermore Christie (1989) states that a typical depth of the lower waveguide is 500 m. A lower waveguide depth of 500 m is then more reasonable than a deep depth of 1200 m. Indeed, for a layer depth $h = 1200$ m, the linear wave speed (6.3) is $764\,\mathrm{m\,s^{-1}}$, which indicates that for large layer depths, resonant flow cannot occur. The high linear wave speed also indicates that modelling the stratification in the lower layer by a constant Brunt–Väisälä frequency is not adequate for large layer depths h. For a lower layer depth of 500 m, $c_1 = 7.4\,\mathrm{m\,s^{-1}}$, which is the flow speed required for exact linear resonance (i.e. $\Delta = 0$). Clark (1984) found that the upper limit on the flow speed for which the morning glory can occur is $7\,\mathrm{m\,s^{-1}}$. Also the numerical calculations of Smith & Noonan (1998) predict an onshore seabreeze of between $4\,\mathrm{m\,s^{-1}}$ and $5\,\mathrm{m\,s^{-1}}$ on the western side of Cape York Peninsula, which for a waveguide depth of $h = 500$ m gives $-1.131 < \Delta < -0.799$ on using (2.5) and (6.1) to (6.3). Now expression (6.4) for the non-dimensional mountain height gives $0.78 \leqslant \sqrt{g_0} \leqslant 1.104$, so that $\Delta = -\sqrt{g_0}$ is a more realistic value of Δ. Indeed, the pressure jumps for this value are in better agreement with the observational data than those for $\Delta = 0$. The modulation solution values for the pressure jump are in general agreement with the observational data for $\Delta = -\sqrt{g_0}$. This is particularly good given that the assumed stratification of the waveguide layer which has been used to generate the predictions is an approximation to the actual waveguide. Also the waveguide has been assumed to have constant properties from the west coast of Cape York Peninsula to the measurement points on the southern side of the Gulf of Carpentaria. It is noted that the morning glory propagates over the sea from its generation region to the measuring regions. Furthermore, a number of other physical effects, such as viscous loss and rotation, have been neglected. In this regard, Christie (1989) examined the effect of viscous loss via numerical solutions

G_0 (m)	Δ	ΔP (hPa)
100	−0.799	0.62
100	−1.131	0.35
150	−0.799	0.90
150	−1.131	0.63
200	−0.799	1.14
200	−1.131	0.87

TABLE 3. Pressure jump ΔP of the lead wave of an upstream wavetrain (morning glory) as given by the modulation solution for a range of mountain heights G_0. Δ calculated from results of Smith & Noonan (1998). Waveguide depth is $h = 500$ m.

of a Burgers–Benjamin–Ono equation. However when viscous loss is included in the Benjamin–Ono equation, the simple structure of the modulation equations is lost and, with it, the possibility of a solution for a damped simple wave (see Smyth 1998 for the equivalent case for the Korteweg–de Vries equation). Clark *et al.* (1981) noted that theoretical estimates of the viscous decay of the morning glory based on assuming that it is a weakly nonlinear wave were far too large to conform with its observed lifetime. Based on their numerical calculations, Smith & Noonan (1998) hypothesized that the longitivity of the morning glory is explained by it being continuously forced by mesoscale circulations over Cape York Peninsula. These circulations have been reduced in the present model to a uniform onshore seabreeze from the Gulf of Carpentaria of speed U.

Like table 2, table 3 lists the pressure jump (6.6) for the lead wave of the upstream modulated wavetrain, but for values of Δ corresponding to the bounds $4\,\mathrm{m\,s^{-1}}$ and $5\,\mathrm{m\,s^{-1}}$ for the onshore seabreeze as predicted from the numerical calculations of Smith & Noonan (1998). Comparing these values with the observational values listed in table 1, we see that the modulation solution is in accord with the observational data, except for the lower bound on the mountain height $G_0 = 100$ m for $\Delta = -1.131$ (for $4\,\mathrm{m\,s^{-1}}$), for which the pressure jump is too low.

The lead wave of the upstream modulated wavetrain is a solitary wave. Therefore from the soliton solution (2.11), the non-dimensional half-width w and velocity v of the lead wave are

$$w = \frac{1}{2(b-c)} \quad \text{and} \quad v = \Delta - 2b. \tag{6.7}$$

Then using the non-dimensionalizations (2.3) and the solution (4.5) for b for $\Delta \leqslant 0$ gives the dimensional half-width W and soliton velocity V as

$$W = \frac{h}{2\left(\frac{1}{2}\Delta + \pi^2\sqrt{G_0/32h}\right)} \quad \text{and} \quad V = -\frac{4N}{\pi}\sqrt{\frac{hG_0}{2}}, \tag{6.8}$$

on noting the parameter values (6.1) to (6.3) and that $c = 0$ for the upstream wavetrain.

In table 4 the lead wave half-widths W and speeds $|V|$ are listed for the same range of mountain heights as in the previous tables and for the upper and lower values of Δ from the numerical calculations of Noonan & Smith (1998), based on a waveguide depth of $h = 500$ m. Noonan & Smith (1985) reported observed morning glory speeds of between $9.6\,\mathrm{m\,s^{-1}}$ and $11.1\,\mathrm{m\,s^{-1}}$ and lead wave half-widths W of between 1500 m and 2000 m and Menhofer *et al.* (1997) reported morning glory speeds of between

G_0 (m)	Δ	$\lvert V\rvert$ (m s^{-1})	W (m)	A_s^*/h
100	−0.799	4.7	657	0.62
100	−1.131	4.7	1165	0.35
150	−0.799	5.7	450	0.90
150	−1.131	5.7	641	0.63
200	−0.799	6.6	355	1.14
200	−1.131	6.6	465	0.87

TABLE 4. Speed $|V|$, half-width W and amplitude to waveguide depth ratio A_s^*/h for the lead wave of an upstream wavetrain (morning glory) as given by the modulation solution for a range of mountain heights G_0. Δ calculated from results of Smith & Noonan (1998). Waveguide depth is $h = 500$ m.

5.2 m s^{-1} and 15.3 m s^{-1}. It can be seen that the modulation theory predicts lead wave speeds towards the lower end of the observed speeds for $G_0 = 150$ m and $G_0 = 200$ m. However for these mountain heights, the half-widths of the lead wave are smaller than the observed half-widths by a factor of between 2 and 5.

Noonan & Smith (1985) assumed that the morning glory consists of Benjamin–Ono solitons. They then used observational data from the region of the southern Gulf of Carpentaria to numerically calculate the modal function ϕ and hence the amplitude, speed and half-width of the solitons. In this manner they found that Benjamin–Ono theory predicted pressure jumps smaller than the observed jumps and half-widths larger than the observed widths by factors of 2 and 3. However the predicted speeds were in rough accord with the observed speeds. To calculate the soliton parameters, Noonan & Smith (1985) had to assume values for A_s^*/h, where A_s^* is the dimensional soliton amplitude, and took $A_s^*/h = 0.2$ and $A_s^*/h = 0.3$. In the present work, these values do not have to be assumed because the amplitude of the modulated wavetrain is determined by the amplitude of the forcing that generates it. Using the soliton amplitude (5.3) and the non-dimensionalizations (2.3), table 4 also lists the values of A_s^*/h for each of the mountain heights. It can be seen that the values of this parameter are much larger than those assumed by Noonan & Smith (1985). This explains why the pressure jumps are larger and the widths are lower in the present work since pressure jumps increase and widths decrease with A_s^*/h. However Benjamin–Ono theory is based on an asymptotic expansion in the small parameter A_s^*/h. Hence the applicability of weakly nonlinear theory is questionable for h of the order of 500 m for larger mountain heights. The questionable applicability of the Benjamin–Ono equation to the morning glory due to A_s^*/h not being small was also noted by Noonan & Smith (1985). For weakly nonlinear theory to be within its range of validity, we need to assume that $G_0/h \ll 1$, which is questionable for a waveguide of depth $h = 500$ m and a mountain height of $G_0 = 200$ m. The application of weakly nonlinear theory outside its range of validity is one reason why the values of W and $|V|$ do not agree with the observations. Another possible reason, pointed out by Noonan & Smith (1985), is that the ratio h/H of the lower layer depth h to the upper layer depth H is not sufficiently small, being of the order of 0.125 for $H = 4$ km (Menhofer *et al.* 1997). This implies that in order to obtain an accurate model of the modulated wavetrain generated by the mountains on Cape York Peninsula, fully nonlinear theory must be used. However, for fully nonlinear theory there is no modulation solution and the only way to proceed is via full numerical solutions of the Euler equations in the Boussinesq approximation.

7. Conclusions

The solution for the resonant (trans-critical) flow of a two-layer fluid over topography in the limit in which the upper layer is much deeper than the lower layer has been obtained. This flow is described by a forced Benjamin–Ono equation and the resonant solution was obtained as a simple wave solution of the modulation equations for the Benjamin–Ono equation. This modulation solution was then used to model the morning glory atmospheric phenomenon of the Gulf of Carpentaria of Queensland, Australia. It was found that while the modulation solution gave pressure jumps in accord with observations, the speed and half-width of the lead wave of the modulated wavetrain were not in accord with measurements. This disagreement is due to a number of factors and approximations, the main ones being: (i) for typical waveguide depths, the ratio of the mountain height to the waveguide depth is $O(0.4)$, which is large for a weakly nonlinear theory to be valid; (ii) the waveguide properties have been assumed to be constant from the area of generation of the morning glory on Cape York Peninsula to the southern Gulf of Carpentaria coast where the observations of the morning glory have been made; and (iii) the interaction between the east and west coast seabreezes on Cape York Peninsula has been neglected (Smith & Noonan 1998). In regard to this last point, the numerical results of Smith & Noonan (1998) show that the morning glory is forced by the east coast seabreeze and this forcing helps explain its longevity.

While the morning glory is not adequately described by the modulation theory solution based on the weakly nonlinear Benjamin–Ono equation, this modulation theory solution does indicate that the resonant interaction between the seabreeze and mountains on the western side of Cape York Peninsula is important as modulation theory predicts that the seabreeze velocities are well within the resonant band. It is expected that such strong interaction will persist even in a fully nonlinear theory. Weakly nonlinear Benjamin–Ono theory then predicts that the morning glory would be generated by the interaction of the west coast seabreeze and the mountains on Cape York Peninsula even in the absence of the east coast seabreeze, even though it would then be weaker and not propagate as far before decaying. The longevity of such a morning glory is, of course, open to question (Smith & Noonan 1998). This strong interaction between the topography and the west coast seabreeze has not been considered in previous work.

REFERENCES

Baines, P. G. 1995 *Topographic Effects in Stratified Flows*. Cambridge University Press.

Benjamin, T. B. 1967 Internal waves of permanent form in fluids of great depth. *J. Fluid Mech.* **29**, 559–592.

Christie, D. R. 1989 Long nonlinear waves in the lower atmosphere. *J. Atmos. Sci.* **46**, 1462–1491.

Christie, D. R. 1992 The morning glory of the Gulf of Carpentaria: a paradigm for non-linear waves in the lower atmosphere. *Austral. Met. Mag.* **41**, 21–60.

Christie, D. R., Muirhead, K. J. & Hales, A. L. 1979 Intrusive density flows in the lower troposphere: a source of atmospheric solitons. *J. Geophys. Res.* **84** (C8), 4959–4970.

Clarke, R. H. 1972 The morning glory: an atmospheric hydraulic jump. *J. Appl. Met.* **11**, 304–311.

Clarke, R. H. 1983*a* Fair weather nocturnal inland wind surges and bores, Part II: Internal atmospheric bores in northern Australia. *Austral. Met. Mag.* **31**, 147–160; and Corrigendum **32**, 53.

Clarke, R. H. 1983*b* The morning glory. *Weatherwise*, June, 134–137.

Clarke, R. H. 1984 Colliding sea-breezes and atmospheric bores: two-dimensional numerical studies. *Austral. Met. Mag.* **32**, 207–226.

Clarke, R. H., Smith, R. K. & Reid, D. G. 1981 The morning glory of the Gulf of Carpentaria: an atmospheric undular bore. *Mon. Weath. Rev.* **109**, 1726–1750.

Dobrokhotov, S. Yn. & Krichever, I. M. 1991 Multiphase solutions of the Benjamin–Ono equation and their averaging. translated from *Matematicheskie Zametki* **49** (6), 42–50.

Fornberg, B. & Whitham, G. B. 1978 A numerical and theoretical study of certain nonlinear wave phenomena. *Phil. Trans. R. Soc. Lond.* A **289**, 373–404.

Grimshaw, R. H. J. & Smyth, N. F. 1986 Resonant flow of a stratified fluid over topography. *J. Fluid Mech.* **169**, 429–464.

Gurevich A. V. & Pitaevskii, L. P. 1974 Nonstationary structure of a collisionless shock wave. *Sov. Phys. JETP* **38**, 291–297.

Jorge, M. C., Minzoni, A. A. & Smyth, N. F. 1999 Modulation solutions for the Benjamin–Ono equation. *Physica D* **132**, 1–18.

Lee, S.-J., Yates, G. T. & Wu, T. Y. 1989 Experiments and analysis of upstream advancing solitary waves generated by moving disturbances. *J. Fluid Mech.* **199**, 569–593.

Menhofer, A., Smith, R. K., Reeder, M. J. & Christie, D. R. 1997 "Morning-Glory" disturbances and the environment in which they propagate. *J. Atmos. Sci.* **54**, 1712–1725.

Noonan, J. A. & Smith, R. K. 1985 Linear and weakly nonlinear internal wave theories applied to "morning glory" waves. *Geophys. Astrophys. Fluid Dyn.* **33**, 123–143.

Smith, R. K. 1988 Waves and bores in the lower atmosphere: the "morning glory" and related phenomena. *Earth-Sci. Rev.* **25**, 1501–1518.

Smith, R. K. & Noonan, J. A. 1998 Generation of low-level mesoscale convergence lines over northeastern Australia. *Mon. Weath. Rev.* **126**, 167–185.

Smyth, N. F. 1987 Modulation theory solution for resonant flow over topography. *Proc. R. Soc. Lond.* A **409**, 79–97.

Smyth, N. F. 1988 Dissipative effects on the resonant flow of a stratified fluid over topography. *J. Fluid Mech.* **192**, 287–312.

Whitham, G. B. 1965 Nonlinear dispersive waves. *Proc. R. Soc. Lond.* A **283**, 238–261.

Whitham, G. B. 1974 *Linear and Nonlinear Waves*. John Wiley and Sons.